

Coupled Soil-Atmosphere Modeling for Expansive Regina Clay

S. Azam* and M. Ito

Environmental Systems Engineering, Faculty of Engineering and Applied Science, University of Regina, Regina, SK S4S 0A2, Canada

Received 22 January 2011; revised 30 August 2011; accepted 20 October 2011; published online 12 March 2012

ABSTRACT. Alternate deformations in the expansive clay have crippled civil infrastructure systems in and around the city of Regina that lies in a semi-arid zone. The main objective of this paper was to develop a soil-atmosphere model for predicting the net water flux and the corresponding volume change in the local expansive soil. A one-dimensional hydrologic model was developed, for a homogeneous soil and no ground water table, by coupling material properties with atmospheric parameters. The use of site coordinates ensured material continuity in a strain-independent framework and soil volume changes were calculated using model results in conjunction with laboratory data. Results showed high water absorption and retention capacities for the investigated soil deposit. Conductive atmospheric conditions during summer gradually desaturated the top 2.5 m layer of the clay that imbibed sporadic rainfall water thereby resulting in volume increases. Cyclic variations in the degree of saturation and the corresponding swelling potential were highest at and near the ground surface and gradually decreased with depth. The highest swelling potential was predicted for late summer and equaled 37%. The model reasonably estimated the soil-atmosphere interactions for the investigated expansive clay and was found to depend on an effective capture of site conditions and material properties. An increased modeling duration can ensure steady state with respect to antecedent moisture.

Keywords: soil-atmosphere modeling, flux regime, expansive clay, climatic parameters

1. Introduction

The adverse effects of soil volume change on engineering construction are multiplied when seasonal climatic variations are significant. This is clearly observed in Regina, Saskatchewan, where alternating movements of the expansive clay has crippled civil infrastructure such as water supply and sewage collection systems (Hu and Hubble, 2005), transportation networks (Kelly et al., 1995) and residential, industrial and commercial facilities (Azam and Ito, 2007). The combined effect of atmospheric parameters results in periodic water deficit and water excess in the surface layer of the clay. This phenomenon leads to recurring swelling and shrinkage in the soil owing to the expansive nature of the local geological deposit. Field monitoring of ground condition such as the measurement of pore water pressure (Vu et al., 2007) and total heave (Yoshida et al., 1983) have been attempted for important construction projects. However, such measurements are generally prohibitive because of the associated sensor installation cost and the long time and huge effort required in analyzing the collected data. Nonetheless, a clear understanding of soil-atmosphere interaction is critical for all types of construction in, on, or with indigenous expansive soils.

The main objective of this paper is to develop a coupled soil-atmosphere model for predicting the net water flux and the corresponding volume change in the expansive Regina clay. First, the model was developed using the following inputs: (i) material properties from laboratory tests on undisturbed soil samples and (ii) boundary conditions obtained from a one-year climate data (from October 1, 2006 to October 1, 2007). Next, the model was validated using measured degree of saturation data from the field. Finally, the estimated degree of saturation was used in conjunction with a laboratory determined swell-shrink curve to estimate the swelling potential (change in height divided by the original height) in the surface layer of the local clay deposit.

2. Literature Review

The hydrologic behavior of an unsaturated soil deposit depends on the following factors: (i) material properties, namely; the soil water characteristic curve (*SWCC*) and the hydraulic conductivity function; (ii) atmospheric parameters such as precipitation, temperature, wind speed, relative humidity, and net radiation; and (iii), geometrical boundary conditions including the ground water table. The interaction of these factors results in suction (difference of air pressure and hydraulic head) variation with depth. Figure 1 gives the conceptual hydrologic model in an unsaturated soil deposit. The unsaturated zone, between the ground surface and the ground water table, can be divided into an active zone and a steady zone. Seasonal climatic variations result in suction fluctuations in the former zone

* Corresponding author. Tel.: +1 306 3372369; fax: +1 306 5854855.
E-mail address: Shahid.Azam@UR Regina.CA (S. Azam).

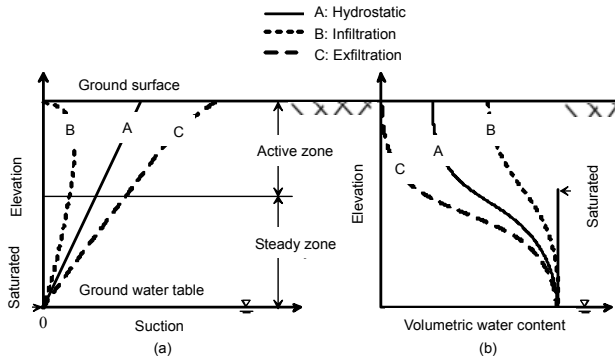


Figure 1. Conceptual hydrologic model for an unsaturated soil deposit: (a) suction profiles and (b) volumetric water content profiles.

whereas the latter zone is independent of time and is primarily influenced by the steady recharge rate and the depth of ground water table (Lu and Likos, 2004).

Figure 1 illustrates three typical hydrologic cases in an unsaturated soil deposit. Under hydrostatic conditions (Curve A), suction varies linearly with depth because of a constant hydraulic head. The corresponding volumetric water content distribution is given by the *SWCC* that shows minimum volumetric water content at the ground surface and complete saturation at the ground water table. During infiltration (Curve B) due to a net water excess such as a rainfall event, water moves downward under an increased hydraulic head. Consequently, suction decreases and volumetric water content increases because of water absorption by the soil. The flow direction is reversed during the opposite process of evaporation (Curve C) that results due to a net water deficit such as a drought event. The rate of water flux (infiltration or exfiltration) governs the extent of shift in both the suction and the volumetric water content profiles from the hydrostatic condition.

The downward water migration phenomenon through unsaturated porous media was first formulated by Richards (1931). Several attempts have been made to develop mathematical solutions to this equation such as by Philip (1969), Swartzendruber (1987), and Ross (1990). These studies primarily focused on understanding the spatial and temporal variation of volumetric water content. Warrick et al. (1990) provided an analytical solution to Richards' equation by incorporating the gravity term in the water flow. To account for desiccation cracks in clays, Beven and Germann (1981) treated the micropores and the macropore as distinct domains and subsequently estimated the combined water flow in their model. Finally, Askar and Jin (2000) simultaneously captured gravity effects, macroporous drainage, and volume changes in an infiltration model for swelling soils.

The upward water movement from an unsaturated soil during evaporation was introduced by Penman (1948). Philip and de Vries (1957) developed a temperature-based method whereas Priestley and Taylor (1972) developed an energy-based method to estimate potential evaporation. These methods assumed that water is freely available at the ground surface for evaporation (that is, complete saturation) thereby predicting a

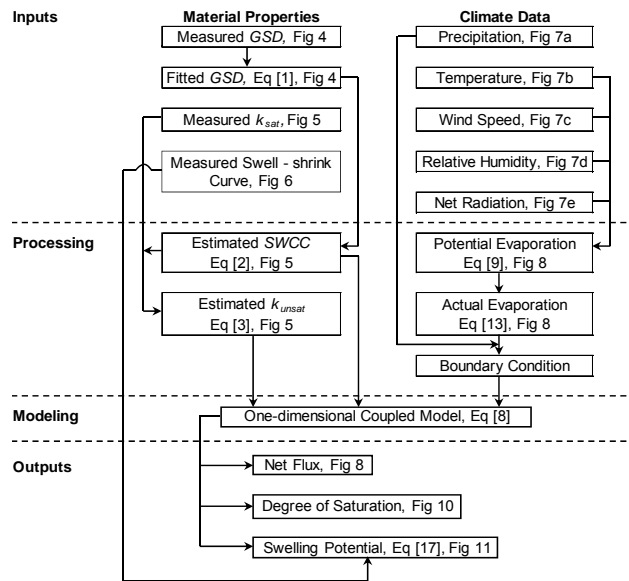


Figure 2. Flow chart of numerical modeling.

maximum potential rate of evaporation. Gray (1970) showed that the ratio of actual to potential evaporation equals 100% (water content at field capacity) for saturated conditions and gradually declines with desaturation reaching the wilting point water content for plants. This relationship was used in the coupled soil-atmosphere model for evaporative fluxes for sands (Wilson et al., 1994) that was subsequently improved to include silts and clays (Wilson et al., 1997). Gitirana et al. (2006) showed that the estimated actual evaporation can be used along with precipitation to evaluate the atmospheric interactions with soils. To date, a robust model including the effect of volume changes and desiccation cracks in swelling soils does not exist.

Material properties are usually assumed to be constant in hydrological modeling. Alternate saturation and desaturation due to seasonal weather variations result in changes in the soil hydraulic properties (Bormann and Klassen, 2008). The current model coupled the soil properties (which vary with the degree of saturation) with the atmospheric parameters described earlier. For expansive clays, cyclic swelling and shrinkage also has a bearing on the hydrologic fluxes (Smiles, 2000). Theoretically, modeling for such soils should satisfy material continuity and account for lateral confinement. Use of material coordinates based on site conditions results in a flow equation analogous to the Richards equation for non-swelling soils. This strain-independent framework was utilized in the present study.

3. Modeling Process

Figure 2 describes the coupled soil-atmosphere modeling process. Homogeneous soil conditions, absence of ground water table up to 10 m depth, and cancelling of swelling movements due to soil load beyond 3 m (Shah, 2011) provided the rationale to develop a one-dimensional model. The model consisted of two input categories, namely: soil properties and

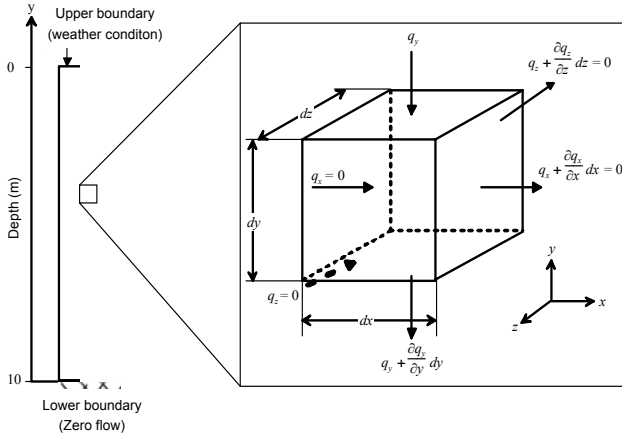


Figure 3. Three-dimensional water flow through an initially unsaturated elemental soil volume.

atmospheric parameters. Material properties included a soil water characteristics curve and a hydraulic conductivity function. The *SWCC* was estimated from the laboratory determined index properties (water content (w), specific gravity (G_s), and dry unit weight (γ_d)) and a grain size distribution (*GSD*) curve. Likewise, the hydraulic conductivity function was obtained from a laboratory measured saturated hydraulic conductivity (k_{sat}) and the estimated *SWCC*. The climate data was used to determine the infiltration flux (precipitation) and the exfiltration flux (temperature, relative humidity, wind speed, and net radiation). The sum of these opposing fluxes was applied as boundary condition to calculate the net flux in relation to material properties. This boundary condition is independent of the swelling and shrinkage behavior of the soil. The model predicted the degree of saturation as a function of time and depth. These data were used in conjunction with a laboratory determined swell-shrink curve to estimate the swelling potential in the surface layer of the local clay deposit.

To mimic *in situ* conditions, the model geometry consisted of a 10 m high homogenous soil column with climate conditions applied at the top and zero water flux applied at the bottom (Figure 3). As the clay deposit has an average depth of 10 m with no ground water table (Ito and Azam, 2009), volume changes were considered to be primarily due to seasonal climatic variations. A one-year daily climate data (from October 1, 2006 to October 1, 2007) was obtained from a weather station at the Regina International Airport. The model had a 10 mm vertical resolution and a 24 hour temporal resolution. The model was validated using measured degree of saturation data from the field. The site for data collection and sample acquisition (for determination of material properties) was chosen to be in the vicinity (at a distance of about 3 km) of the weather station.

4. Governing Equations

4.1. Material Properties

The *SWCC* was estimated from measured index properties (w , G_s , and γ_d) and *GSD*. To obtain a smooth curve, the

laboratory determined *GSD* data was fitted by the following Pedo-Transfer Function, $P_p(d)$, (Fredlund et al., 2002):

$$P_p(d) = \frac{1}{\ln \left[\exp(1) + \left(\frac{a_{gr}}{d} \right)^{n_{gr}} \right]^{m_{bi}}} \left\{ 1 - \frac{\left[\ln \left(1 + \frac{d_r}{d} \right) \right]^7}{\left[\ln \left(1 + \frac{d_r}{d_m} \right) \right]^7} \right\} \quad (1)$$

The following fitting parameters ($a_{gr} = 0.003068$, for the initial break point of the curve; $n_{gr} = 1.571434$, for the steepest slope of the curve; $m_{bi} = 0.948263$, for the shape of the fines part of the curve; and $d_r = 0.001$, for the amount of fines in soil) and grain sizes (d , that under consideration and $d_m = 0.00001$, the minimum allowable) were used. The fitted *GSD* curve was divided into smaller groups of nearly same size grains and a unique *SWCC* was obtained for each group using the following equation (Fredlund and Xing, 1994):

$$w_w = w_s \left[1 - \frac{\ln \left(1 + \frac{\psi}{h_r} \right)}{\ln \left(1 + \frac{10^6}{h_r} \right)} \right] \left[\frac{1}{\left\{ \ln \left[\exp(1) + \left(\frac{\psi}{a_f} \right)^{n_f} \right] \right\}^{m_f}} \right] \quad (2)$$

The above equation included gravimetric water contents (w_w , any value and w_s , saturated value), fitting parameters ($a_f = 1354.058$, for air entry value; $n_f = 0.833822$, for soil desaturation rate; $m_f = 0.940235$, for function curvature at high suction) and $h_r = 49940.34$, that is a constant representing soil suction (ψ) at the residual water content. The sum of the *SWCC* segments generated the entire *SWCC* that, along with the measured k_{sat} (Table 1), was used to determine the unsaturated hydraulic conductivity function ($k_r(\psi)$). Denoting $\ln(10^6)$ by b , a dummy integration variable by y , volumetric water content by θ , and air entry value by a_f , the following equation was used (Fredlund et al., 1994):

$$k_r(\psi) = \frac{\int_{\ln(\psi \text{ at } a_f)}^b \frac{\theta(e^y) - \theta(\psi)}{e^y} \theta'(e^y) dy}{\int_{\ln(\psi \text{ at } a_f)}^b \frac{\theta(e^y) - \theta_s}{e^y} \theta'(e^y) dy} \quad (3)$$

4.2. Water Flow

To derive an equation for saturated-unsaturated seepage through a soil element ($V_o = dx.dy.dz$, m^3), the law of mass conservation was written in one-dimensional form. Figure 3 explains the three-dimensional water flow through an initially unsaturated elemental soil volume. Water flow in the x and the z directions was neglected because of the homogenous nature of the soil. In the absence of a ground water table up to 10 m

depth, water flow was predominantly in the y direction. Using q_y^w and q_y^v for mass flux rates of liquid and vapor water in y direction (vertical) per unit area, $\text{kg}/(\text{m}^2\text{s})$, respectively; M_w for mass of soil water, kg ; and t for time, s ; the following equation was developed (Fredlund and Rahardjo, 1993):

$$-\frac{\partial}{\partial y}(q_y^w + q_y^v) = \frac{1}{V_o} \frac{\partial M_w}{\partial t} \quad (4)$$

Denoting volumetric water content by V_w/V_o , void ratio by e , degree of saturation by S , and suction by $(u_a - u_w)$, the coefficient of water storage (m_2^w) was calculated as the slope of the *SWCC* using the following equation (Fredlund and Rahardjo, 1993):

$$m_2^w = \frac{d(V_w/V_o)}{d(u_a - u_w)} = \frac{e}{1+e} \frac{dS}{d(u_a - u_w)} \quad (5)$$

Similarly, denoting the flow rate of liquid pore water in the y direction across a unit area of soil by v_y^w , m/s ; hydraulic conductivity function by $k_y^w(\theta)$; hydraulic gradient by $\partial h/\partial y$; and hydraulic head by h , m ; the generalized one-dimensional Darcy's law was written as follows:

$$v_y^w = -k_y^w(\theta) \frac{\partial h}{\partial y} \quad (6)$$

Water vapor flow through unsaturated soils occurs under a vapor concentration gradient. Assuming a thermodynamic equilibrium to represent a negative pore water pressure as the vapor gradient, a modified form of Fick's law expressing the water vapor flow was written as follows (Dakshnamurthy and Fredlund, 1981):

$$v_y^v = \frac{k^{vd}(\theta) \partial u_w}{\gamma_w \partial y} \quad (7)$$

where $k^{vd}(\theta)$ is pore water vapour conductivity in air, m/s ($k^{vd} = \gamma_w (W_v p_v / (\rho_w R(T + 273.15))) (D^{v*} / \rho_w)$), W_v is molecular weight of water vapor, 18.016 kg/kmol ; p_v is partial pressure of water vapor, kPa ; R is universal gas constant, 8.314 J/kmol ; T is temperature, $^\circ\text{C}$; D^{v*} is vapour diffusivity through soil, $(\text{kg}\cdot\text{m})/(\text{kN}\cdot\text{s})$, ρ_w is unit weight of water; and u_w is pore water pressure in the y direction.

Combining Equations (4), (5), (6), and (7), the transient saturated-unsaturated seepage through porous media was described according to the following equation (Wilson, 1997):

$$\frac{\partial}{\partial y} \left[(k_y^w(\theta) + k^{vd}(\theta)) \frac{\partial h}{\partial y} - k^{vd}(\theta) \right] = -\gamma_w m_2^w \frac{\partial h}{\partial t} \quad (8)$$

Equation (8) shows that the flow entering and leaving a unit volume is equal to the volumetric water content. This relationship assumes that water is incompressible and that there is no volume change in soils (V_o is constant) due to loading and unloading because pore air pressure is constant under atmospheric conditions. Therefore, the only source causing fluctua-

tions in volumetric water content is the soil suction. The numerical value of soil suction is obtained from the *SWCC* slope that describes a smooth transition between saturated and unsaturated soils. Since V_o changes due to water flow through expansive soils, volume changes should be calculated using the model in conjunction with a laboratory measured swell-shrink curve.

4.3. Climate Data

Surface conditions were identified to solve the governing equations. The following modified Penmen method was used to transform climate data to infiltration and evaporation fluxes at the soil surface thereby calculating potential evaporation (*PE*) per unit time, m/day (Gitirana et al., 2006):

$$PE = \frac{\Delta Q_N + E_a \gamma}{\Delta + \gamma} \quad (9)$$

where Δ is slope of the saturation vapour pressure curve with respect to temperature, $\text{mmHg}/^\circ\text{F}$; Q_N is heat budget, m/day ; E_a is a parameter, m/day ($E_a = f(u) p_{vsat}^{air} (1 - RH_a)$) that depends on vapour pressure of air above surface (p_{vsat}^{air} , mm Hg), wind speed (U_a , m/day given by $f(u) = 0.35 (1 + 0.15U_a)$) and relative humidity of air, RH_a); and γ is psychrometer constant, $0.27 \text{ mm Hg}/^\circ\text{F}$.

A series of constants ($a_0 = 0.61835380754$, $a_1 = 0.041142732$, $a_2 = 0.0017217473$, $a_3 = 0.000074108$, $a_4 = 0.0000003985$, and $a_5 = 0.0000000022$) and atmospheric air temperature (T_a , $^\circ\text{C}$) data were used to calculate Δ and p_{vsat}^{air} as follows (Lowe, 1977):

$$\Delta = a_1 + 2a_2 T_a + 3a_3 T_a^2 + 4a_4 T_a^3 + 5a_5 T_a^4 + 6a_5 T_a^5 \quad (10)$$

$$p_{vsat}^{air} = a_0 + a_1 T_a + a_2 T_a^2 + a_3 T_a^3 + a_4 T_a^4 + a_5 T_a^5 + a_6 T_a^6 \quad (11)$$

Similarly, denoting reflection coefficient by r ; short wave radiation by R_c , m/day (given by $0.95 R_a (0.18 + 0.55 n/N)$); solar radiation by R_a , $\text{MJ}/\text{m}^2/\text{day}$; sunshine ratio by n/N ; and Boltzman's constant by σ , $\text{W}/\text{m}^2/\text{K}^4$; the heat budget was calculated as follows (Lowe, 1977):

$$Q_N = (1-r)R_c - \sigma T_a^4 (0.56 - 0.092(p_{vsat}^{air})^{0.5}) (0.10 + 0.90 n/N) \quad (12)$$

From the potential evaporation, the actual evaporation (*AE*, m/day) was calculated using the following limiting function in SVFlux (Wilson, 1997):

$$AE = PE \left(\frac{p_v - p_v^{air}}{p_{vsat} - p_v^{air}} \right) = PE \left(\frac{RH_s - \left(\frac{p_{vsat}^{air}}{p_{vsat}} \right) RH_a}{1 - \left(\frac{p_{vsat}^{air}}{p_{vsat}} \right) RH_a} \right) \quad (13)$$

Table 1. Summary of Geotechnical Properties

Property	ASTM Test Method	July 2007	August 2007
		0.9 m Depth	0.6 m Depth
Field Gravimetric Water Content, w (%)	D2216-10	34.2	31.2
Field Dry Unit Weight, γ_d (kN/m ³)	D2937-10	13.5	13.4
Field Volumetric Water Content, θ (%)	/	47.0	43.0
Specific Gravity, G_s	D854-10	2.80	2.75
Field Void Ratio, e	/	1.03	1.0
Degree of Saturation, S (%)	/	93.0	84.0
Liquid Limit, w_l (%)	D4318-10	77.8	82.8
Plastic Limit, w_p (%)	D4318-10	27.0	30.1
Plasticity Index, I_p (%)	D4318-10	50.8	52.7
Saturated Hydraulic Conductivity, k_{sat} (m/s)	D2435-04	5×10^{-9}	5×10^{-9}

* $\theta = (\gamma_d / \gamma_w) w$, $e = (G_s / \gamma_d) - 1$, $S = w G_s / e$, $I_p = w_l - w_p$ (where, $\gamma_w = 9.81 \text{ kN/m}^3$).

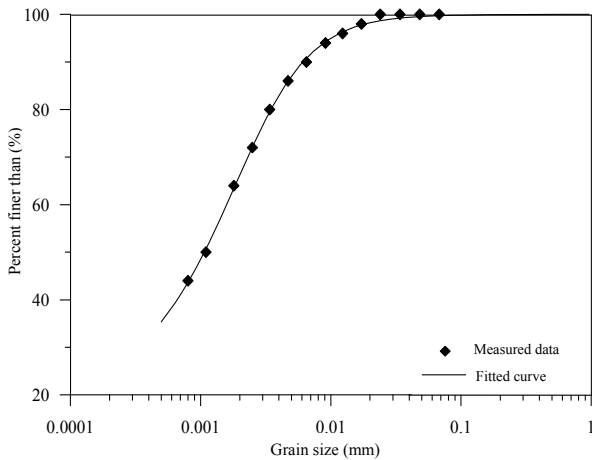


Figure 4. Grain size distribution.

where p_v , p_v^{air} and p_{vsat} are vapour pressures (kPa) of the material surface, of air near ground, and under complete saturation, respectively, and RHs is relative humidity at the material surface.

5. Material Properties-Model Input

The undisturbed samples were retrieved from an extensive deposit of the expansive Regina clay according to the ASTM Standard Practice for Thin-walled Tube Sampling of Soils for Geotechnical Purposes (D1587-08). To preserve the field water content, the samples were wrapped with plastic sheets and coated with molten wax in accordance with the ASTM Standard Practice for Preserving and Transporting Rock Core Samples (D5079-08). All of the samples were transported to the Geotechnical Testing Laboratory at the University of Regina and stored at 24°C in a humidity chamber.

Table 1 summarizes the index properties of Regina clay indicating the soil type and its field condition. The data indicate that the top 1.0 m layer of the deposit readily responds to atmospheric conditions. Due to snow melt in spring and rainfall in early summer, the degree of saturation measured 93% at 0.9 m depth and dropped to 84% (at a shallower depth of 0.6 m) after a summer month. These measurements were con-

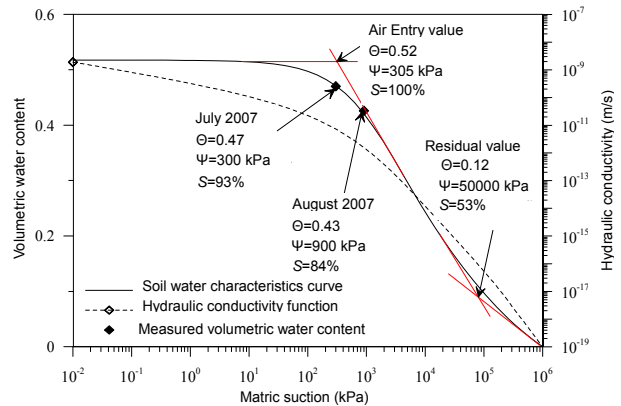


Figure 5. Soil water characteristics curve and hydraulic conductivity function.

sidered sufficient owing to a slow water movement in the soil. The high liquid limit ($w_l \approx 80\%$) and plastic limit ($w_p \approx 28\%$) suggest high water absorbing and retaining capacity for the investigated clay. These data corroborate well with the reported mineralogical composition of the clay. According to Ito and Azam (2009), expansive clay minerals such as smectite, hydrous mica, and chlorite are the primary constituents of the native soil.

Figure 4 illustrates the grain size distribution curve for the investigated soil. The measured data fitted well to a uni-model curve according to Equation (1). The soil was found to be mainly fine-grained with about 99% of the material finer than 0.0075 mm and about 66% clay size fraction, C (material finer than 0.002 mm). The corresponding activity ($A = I_p / C = 0.8$) indicate that the engineering behaviour of the investigated clay should be similar to the illite clay mineral that is known to have a moderate swelling capability (Azam and Ito, 2007).

Figure 5 gives the *SWCC* and the hydraulic conductivity function. The curve comprises of three straight-line portions, which can be determined using four points: (i) saturated condition (obtained from laboratory measurements); (ii) air entry value; (iii) residual condition; and (iv) dry condition (theoretically the same for all soil types (Fredlund and Rahardjo, 1993). Therefore, the two inflection points are sufficient to determine

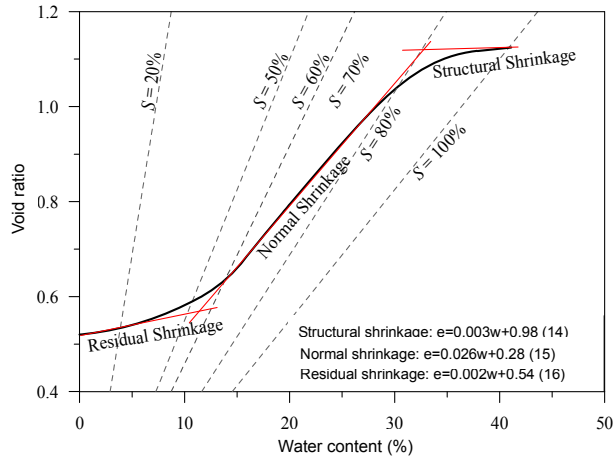


Figure 6. Swell-shrink curve.

the shape of the *SWCC* curve. The estimated *SWCC* curve showed an air entry value of 305 kPa and a residual suction of 50000 kPa at volumetric water contents of 0.52 and 0.13, respectively. Pertaining to inflection points on the curve, these values were obtained by drawing lines tangential to the three straight-line portions of the curve. Physically, the air entry value is that at which desaturation commences through the intrusion of air into the soil pores whereas the residual value is that at which vapour phase transport becomes the primary water migration mechanism. The *SWCC* shape and critical values on the curve corroborated well with published data for Regina clay such as by Khanzode et al. (2002). The field samples with measured volumetric water contents of 0.47 (July 2007) and 0.43 (August 2007) were used to determine the corresponding suction values. Closely matching with those determined by Vu et al. (2007), these latter values (300 kPa and 900 kPa, respectively) were, in turn, used to determine appropriate initial conditions for the model. In the absence of a ground water table and a corresponding reduction in suction up to the 10 m depth, this range was considered to reasonably approximate the suction variation throughout the soil profile.

The saturated hydraulic conductivity was determined in a fixed ring odometer. The instrument had a brass ring (60 mm internal diameter and 20 mm height) for holding the soil sample between two porous stones and a brass cell (100 mm internal diameter and 40 mm height) that contained water. The k_{sat} was found to be 5×10^{-9} m/s that is typical for clays (Holtz and Kovacs, 1981). The clay generally kept the saturated hydraulic conductivity up to the air entry value. Thereafter, the hydraulic conductivity dropped sharply with increasing suction: a drop of ten orders of magnitude (from 10^{-9} to 10^{-19} m/s) was recorded with a change in the degree of saturation from 100 to 0%.

Figure 6 presents the laboratory determined swell-shrink curve for Regina clay superimposed on theoretical degree of saturation lines obtained from basic phase relationships (Ito and Azam, 2010). The curve comprised of an initial low structural shrinkage followed by a sharp decline during normal shrinkage and then by a low decrease during residual shrinkage (Haines, 1923). During structural shrinkage, some of the

larger and relatively stable voids are emptied such that the decrease in soil volume is less than the volume of water lost. During normal shrinkage, volume decrease in soil is equal to the volume of water lost thereby leading to a 45° straight line parallel to the 100% saturation line. During residual shrinkage, air enters the pores close to the shrinkage limit and pulls the particles together due to suction and leading to a further decrease in soil volume albeit lower than the volume of water lost. In Figure 6, a linear equation (Equations (14), (15), and (16)) was assigned to each of the straight-line component of the swell-shrink curve. These equations were used in conjunction with the model-predicted degree of saturation to determine the initial field void ratio (e_o): the maximum possible void ratio (e_{max}) for Regina clay was found to be 1.1 (Ito and Azam, 2010). The swelling potential (*SP*) was calculated from the following equation:

$$SP = (e_{max} - e_o) / (1 + e_o) \quad (17)$$

6. Climate Data-Model Input

Figure 7 gives the climate data from October 1, 2006 through October 1, 2007. With minor variations, the data generally followed the long-term average values for the area that is classified as a semi-arid zone (BSk) according to the Köppen Climate Classification System (McKnight and Hess, 2001). As depicted in Figure 7a, the total precipitation measured 315 mm and bulk of the rainfall was found to be in the summer months with several storm events. The accumulated winter snow (53 mm) gradually melted in early spring and the process was completed on April 12, 2007, when the temperature peaked to 7.5 °C and remained above freezing for most of the day. Figure 7b indicates that the mean temperature for the year was 3.1 °C but varied extensively from -7.4 °C (October to March) to 13.8 °C (April to September): the maximum difference between the high and low temperatures was 57.4 °C. The wind speed (Figure 7c) was found to be independent of the time of the year and varied between 6 and 44 km/hour with an average value of 19 km/hour. The relative humidity data (Figure 7d) illustrated a high average of 80% during winter and a low average of 65% during summer. The high fluctuations in relative humidity values (with a minimum of 34% and a maximum of 94%) were found to be during the summer time and can be associated with periods of no rainfall and precipitation events. Similarly, the net radiation data (Figure 7e) showed a winter average of 6.4 MJ/m²/day and a summer average of 13.8 MJ/m²/day.

The above data means that during the summer time, the average temperature remained high (13.8 °C), the average wind speed was consistent (19 km/hour), the average relative humidity was low (65%), and the average net radiation was high (13.8 MJ/m²/day). Such conditions generally render the surface layer of Regina clay desiccated. Therefore, in any sporadic rainfall event during the summer, the expansive clay can readily adsorb all of the available water thereby resulting in swelling.

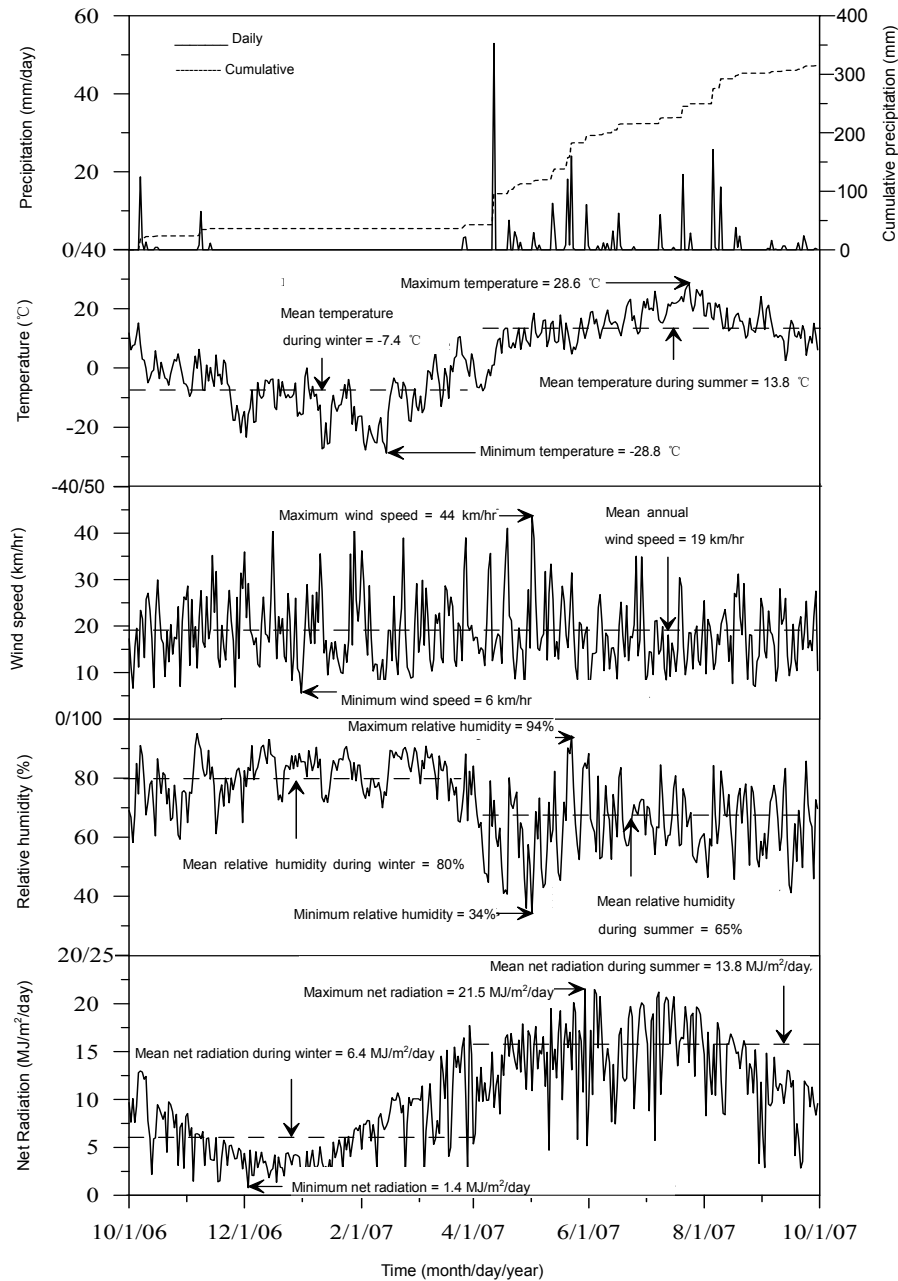


Figure 7. Daily climate data variations with time.

Figure 8 presents the computed cumulative fluxes at the soil-atmosphere interface. The potential evaporation was computed using Equation (9) along with the climate data. The resulting value was, in turn, used to calculate actual evaporation and the difference of precipitation and actual evaporation was registered as the net flux boundary.

7. Soil Response-Model Output

In Figure 8, the negative value of the cumulative net flux indicates that similar to the long-range trend, evaporation ex-

ceeded precipitation in 2006 ~ 2007. Started on October 1, 2006, the model output data exhibited negligible variations until April 2007. To simulate field conditions, a zero net flux was ensured for this duration. This is because precipitation was received as snow (that piled up on the ground and did not infiltrate) and evaporation (measured data not available) was negligible mainly due to a low atmospheric temperature and a high relative humidity. Thereafter, the cumulative net flux gradually decreased because the high amount of total precipitation was offset by the cumulative evaporation due to favorable climatic conditions. Overall, fluctuations in each of the flux

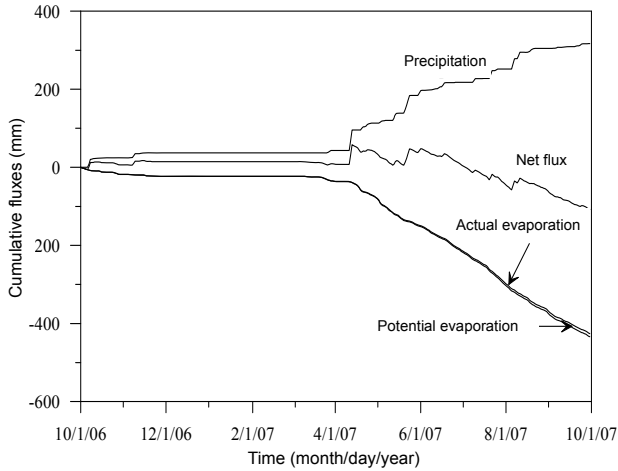


Figure 8. Cumulative simulated fluxes with respect to time.

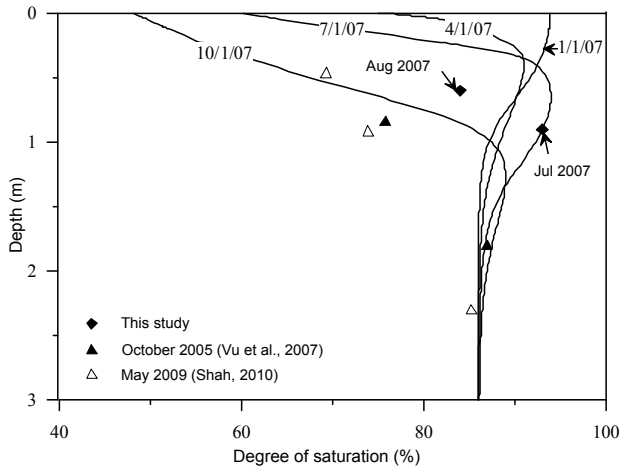


Figure 9. Comparison of model simulations with observed data.

became active around April 2007 because of higher rate of storm events. Therefore, the soil response was analyzed from April 1, 2007 to October 1, 2007.

Figure 9 compares the model simulations with observed data for the entire year. The predicted degree of saturation profiles are shown at a three-month interval. The degree of saturation was found to vary with both depth and time. At surface, the degree of saturation decreased from 94% in January 2007 to 48% in October 2007. This range gradually narrowed down and diminished at about 2.5 m depth. The measured data from this study (July 2007 and August 2007) and those from Vu et al. (2007) for October 2005 corroborated well with the model predictions. However, the observed May 2009 data from Shah (2011) showed that the model over-predicted the degree of saturation, particularly in the top 1 m depth. This is attributed to the combined influence of the following: (i) applying the initial suction value from a different site with possibly different material properties; and (ii) applying the climatic conditions of 2007 to 2009. Clearly, the current model depends on an effective capture of site conditions and material properties. Likewise, an increased modeling du-

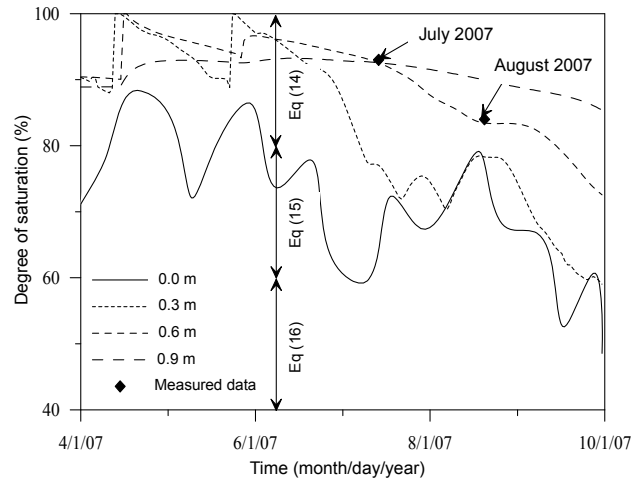


Figure 10. Degree of saturation with respect to time and depth.

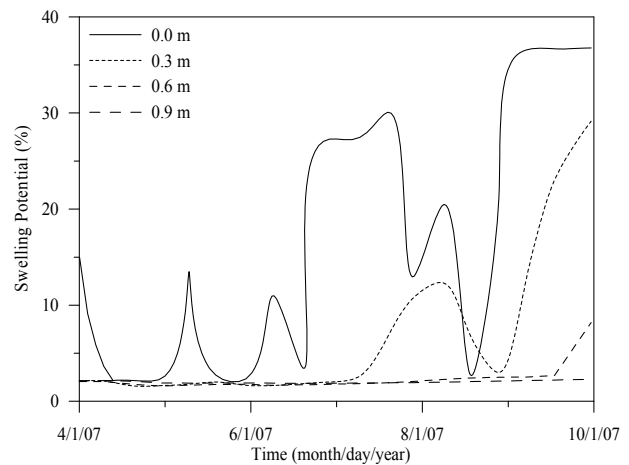


Figure 11. Swelling potential variation with respect to depth and time

ration can ensure steady state with respect to antecedent conditions.

Figure 10 presents the variation in the degree of saturation (weekly average values) over the summer months at selected depths obtained from the vertical model resolution: ground surface (0.0 m), near surface (0.3 m), and sample acquisition depth (0.6 and 0.9 m). For all depths, the degree of saturation was found to generally decrease from April 2007 through October 2007 because of a decreasing net flux. Conversely, the degree of saturation increased with increasing depth such that the fluctuations were predominant at the surface and approached minimum values at 0.9 m. This is attributed to the interaction of atmospheric conditions with the local expansive soil. The surface layer at an initially unsaturated state readily imbibes any water made available by a rainfall event. Likewise, this layer can rapidly lose water under the hot and dry conditions prevalent in the area. With increasing depth, the overlying soil provides a cover and the geotechnical properties of the underlying materials become progressively more significant. The high water retention capability and the low hydrau-

lic conductivity of the clay, especially under unsaturated conditions, impede variations in the degree of saturation at higher depths. These soil-atmosphere interactions corroborated well the observed degree of saturation values obtained at different times and depths thereby validating the numerical modeling output in terms of the engineering behaviour of Regina clay. Overall, the top 2.5 m depth of this expansive soil was found to be the active zone of alternate saturation and desaturation.

Figure 11 gives the predicted swelling potential between April 1, 2007 and October 1, 2007 as a function of time and depth. As mentioned before, the *SP* values were obtained for different depths using appropriate equations (Equations (14), (15), and (16)) from Figure 6 in conjunction with the degree of saturation values from Figure 10. In contrast to the degree of saturation, the *SP* variation was found to increase over time as the soil gradually became more deficient in net water and, consequently, more susceptible to volume increase in case of rainfall events. As expected, the cyclic variation of *SP* generation was highest at and near the ground surface and gradually decreased with depth. The maximum *SP* values for 0.0, 0.3, 0.6, and 0.9 m depths were 37, 30, 12, and 3%, respectively. According to Brown (1984), only 3% of swelling potential can cause damages to lightly loaded structures. For municipal infrastructure (such as roads, walkways, water supply, and sewage collection) and residential construction (especially, basements and driveways), the structural loads are not sufficient to offset the swelling movement of the supporting expansive soil. Therefore, the developed model is in general agreement with the observed soil volume changes in Regina.

8. Summary and Conclusions

The soil-atmospheric flux regime is governed by material properties, seasonal climatic variations and boundary conditions. Given homogeneous conditions and the absence of ground water table up to 10 m depth, a one-dimensional hydrologic model was developed for the expansive Regina clay. The model investigated saturation (due to infiltration) and desaturation (due to evaporation) of the soil by coupling material properties with atmospheric parameters. The use of site coordinates ensured material continuity in a strain-independent framework. Soil volume changes were calculated using the model in conjunction with a laboratory measured swell-shrink curve. The model reasonably estimated the soil-atmosphere interactions for the investigated expansive clay and was found to depend on an effective capture of site conditions and material properties. Likewise, an increased modeling duration can ensure steady state with respect to antecedent moisture. Based on the laboratory determined soil properties, the 2007 climate data, and the specified site conditions, the main results of this research can be concluded as follows:

1. Regina clay possesses high water absorption and retention capacities as indicated by an air entry value of 305 kPa and a residual suction of 50000 kPa at volumetric water contents of 0.52 and 0.13, respectively. The hydraulic conductivity changed by ten orders of magnitude (from 10^{-9} to 10^{-19} m/s) due to complete theoretical desaturation.

2. High temperature, consistent wind speed, low relative humidity, and high net radiation during summer render the surface layer of Regina clay desiccated and ready to imbibe water in any sporadic rainfall event thereby resulting in swelling. The top 2.5 m layer of the clay was found to be the active zone of soil-atmosphere interactions.

3. Cyclic variations in the degree of saturation and the corresponding *SP* were highest at the ground surface and gradually decreased with depth. At 0.9 m depth, the swelling potential was found to be 3%, enough to cause damages to lightly loaded structures.

4. The degree of saturation generally decreased over the summer months because of a decreasing net flux and resulted in a corresponding increase in *SP* during a rainfall event. The highest *SP* was predicted to be 37% in late summer.

Acknowledgments. The financial support from the Natural Science & Engineering Research Council of Canada and the Mathematics of Information Technology & Complex Systems Inc., Canada is gratefully acknowledged. Thanks to the Saskatchewan Ministry of Highways & Infrastructure for providing materials and the University of Regina for providing laboratory space and computing facilities.

References

- Askar, A., and Jin, Y.C. (2000). Macroporous drainage of unsaturated swelling soil, *Water Resour. Res.*, 36(5), 1189-1197. <http://dx.doi.org/10.1029/2000WR900023>
- Azam, S., and Ito, M. (2007). A study on the evaluation of swelling potential of Regina clay modified with sand, *Proc., 60th Canadian Geotechnical Conference*, Ottawa, ON, Canada, 1907-1912.
- Beven, K., and Germann, P. (1981). Water flow in soil macropores, II, a combined flow model, *J. Soil Sci.*, 32(1), 15-29. <http://dx.doi.org/10.1111/j.1365-2389.1981.tb01682.x>
- Bormann, H., and Klassen, K. (2008). Seasonal and land use dependent variability of soil hydraulic and soil hydrological properties of two Northern German soils, *Geoderma*, 145(3-4), 295-302. <http://dx.doi.org/10.1016/j.geoderma.2008.03.017>
- Brown, R.W. (1984). Residential Foundations, Van Nostrand Reinhold, NY, USA.
- Dakshnamurthy, V., and Fredlund, D.G. (1981). A mathematical model for predicting moisture flow in an unsaturated soil under hydraulic and temperature gradients, *Water Resour. Res.*, 17(3), 714-722. <http://dx.doi.org/10.1029/WR017i003p00714>
- Fredlund, D.G., and Rahardjo, H. (1993). *Soil Mechanics for Unsaturated Soils*. Wiley, NY, USA. <http://dx.doi.org/10.1002/9780470172759>
- Fredlund, D.G., and Xing, A. (1994). Equation for the soil-water characteristics curve, *Can. Geotech. J.*, 31(4), 521-532. <http://dx.doi.org/10.1139/t94-061>
- Fredlund, D.G., Xing, A., and Huang, S. (1994). Predicting the permeability function for unsaturated soil using the soil-water characteristics curve, *Can. Geotech. J.*, 31(4), 533-546. <http://dx.doi.org/10.1139/t94-062>
- Fredlund, M.D., Wilson, G.W., and Fredlund, D.G. (2002). Use of the grain-size distribution for estimation of the soil-water characteristic curve, *Can. Geotech. J.*, 39(5), 1103-1117. <http://dx.doi.org/10.1139/t02-049>
- Gitirana, G. Jr., Fredlund, M.D., and Fredlund, D.G. (2006). Numerical modeling of soil-atmosphere interaction for unsaturated surfaces, 4th International Conference on Unsaturated Soils, Care-

- free, AZ, USA, 1, 658-669.
- Gray, D.M. (1970). Handbook on the Principals of Hydrology. Canadian National Committee for the International Hydrological Decade, National Research Council of Canada, Ottawa.
- Haines, W.B. (1923). The volume change associated with variations of water content in soil, *J. Agric. Sci.*, 13(3), 296-310. <http://dx.doi.org/10.1017/S0021859600003580>
- Holtz, W.G., and Kovacs, W.D. (1981). An Introduction to Geotechnical Engineering, Prentice-Hall Inc., Englewood Cliffs, NJ, USA.
- Hu, Y., and Hubble, D.W. (2005). Failure conditions of asbestos cement water mains in Regina, Proc., 33rd Annual Conference of the Canadian Society of Civil Engineering, Toronto, ON, Canada, 1-10.
- Ito, M., and Azam, S. (2009). Engineering characteristics of a glaciolacustrine clay deposit in a semi-arid climate, *B. Eng. Geol. Environ.*, 68(4), 551-557. <http://dx.doi.org/10.1007/s10064-009-0229-7>
- Ito, M., and Azam, S. (2010). Determination of swelling and shrinkage properties of undisturbed expansive soils, *Geotech. Geol. Eng.*, 28(4), 413-422. <http://dx.doi.org/10.1007/s10706-010-9301-0>
- Kelly, A.J., Sauer, E.K., Barbour, S.L., Christiansen, E.A., and Widger, R.A. (1995). Deformation of the Deer Creek bridge by an active landslide in clay shale. *Can. Geotech. J.*, 32(4), 701-724. <http://dx.doi.org/10.1139/t95-069>
- Khanzode, R.M., Vanapalli, S.K., and Fredlund, D.G. (2002). Measurement of soil-water characteristics curves for fine-grained soils using a small-scale centrifuge. *Can. Geotech. J.*, 39(5), 1209-1217. <http://dx.doi.org/10.1139/t02-060>
- Lowe, P.R. (1977). An approximate polynomial for the computation of saturation vapor pressure. *J. Appl. Meteorol.*, 16(1), 100-103. [http://dx.doi.org/10.1175/1520-0450\(1977\)016<0100:AAPFTC>2.0.CO;2](http://dx.doi.org/10.1175/1520-0450(1977)016<0100:AAPFTC>2.0.CO;2)
- Lu, N., and Likos, W.J. (2004). Unsaturated Soil Mechanics, Wiley, NY, USA.
- McKnight, T.L., and Hess, D. (2001). Physical Geography: A Landscape Appreciation, 7th ed. Prentice-Hall Inc., Englewood Cliffs, NJ, USA.
- Penman, H.L. (1948). Natural evapotranspiration from open water, bare soil and grass, *Proc. R. Soc. Lond., Ser. A*, 193, 120-146. <http://dx.doi.org/10.1098/rspa.1948.0037>
- Philip, J.R. (1969). Hydrostatics and hydrodynamics in swelling soils, *Water Resour. Res.*, 5(5), 1070-1077. <http://dx.doi.org/10.1029/WR005i005p01070>
- Philip, J.R., and de Vries, D.A. (1957). Moisture movement in porous materials under temperature gradients. *Trans. Amer. Geophys. Union.*, 38(2), 222-232.
- Priestley, C.H.B., and Taylor, R.J. (1972). On the assessment of surface heat flux and evaporation using large-scale parameters, *Mon. Weather Rev.*, 100(2), 81-92. [http://dx.doi.org/10.1175/1520-0493\(1972\)100<0081:OTAOSH>2.3.CO;2](http://dx.doi.org/10.1175/1520-0493(1972)100<0081:OTAOSH>2.3.CO;2)
- Richards, L.A. (1931). Capillary conduction of liquids through porous medium. *J. Appl. Physics.*, 1(5), 318-333. <http://dx.doi.org/10.1063/1.1745010>
- Ross, P.J. (1990). Efficient numerical methods for infiltration using Richards' equation. *Water Resour. Res.*, 26(2), 279-290. <http://dx.doi.org/10.1029/WR026i002p00279>
- Shah, I. (2011). *Swelling Properties of an Unsaturated Expansive Soil Deposit*. M.A.Sc. Thesis. University of Regina, SK, Canada.
- Smiles, D.E. (2000). Hydrology of swelling soils: a review. *Aust. J. Soil Res.*, 38(3), 501-521. <http://dx.doi.org/10.1071/SR99098>
- Swartzendruber, D. (1987). A quasi-solution of Richards' equation for the downward infiltration of water into soil. *Water Resour. Res.*, 23(5), 809-817. <http://dx.doi.org/10.1029/WR023i005p00809>
- Vu, H.Q., Hu, Y., and Fredlund, D.G. (2007). Analysis of Soil Suction Changes In Expansive Regina Clay. *Proc. 60th Canadian Geotechnical Conference*, Ottawa, ON, Canada, 1069-1076.
- Warrick, A.W., Lomen, D.O., and Islas, A. (1990). An analytical solution to Richards' equation for a draining soil profile. *Water Resour. Res.*, 26(2), 253-258. <http://dx.doi.org/10.1029/WR026i002p00253>
- Wilson, G.W. (1997). Surface flux boundary modeling for unsaturated soils. Unsaturated Soils Engineering Practice, Geotechnical Special Publication No. 68, ASCE, 38-65.
- Wilson, G.W., Fredlund, D.G., and Barbour, S.L. (1994). Coupled soil-atmosphere modeling for soil evaporation. *Can. Geotech. J.*, 31(2), 151-161. <http://dx.doi.org/10.1139/t94-021>
- Wilson, G.W., Fredlund, D.G., and Barbour, S.L. (1997). The effect of soil suction on evaporative fluxes from soil surfaces. *Can. Geotech. J.*, 34(1), 145-155. <http://dx.doi.org/10.1139/t96-078>
- Yoshida, R., Fredlund, D.G., and Hamilton, J.J. (1983). The prediction of total heave of a slab-on-grade floor on Regina clay. *Can. Geotech. J.*, 20(1), 69-81. <http://dx.doi.org/10.1139/t83-008>